

# One-Forcing: Towards Stable One-Step Autoregressive Video Generation

Jiaqi Feng<sup>1\*</sup> Justin Cui<sup>2\*</sup> Yuanhao Ban<sup>2</sup> Cho-Jui Hsieh<sup>2</sup>  
<sup>1</sup>Tsinghua University <sup>2</sup>UCLA

Project Page: <https://aurora-edu.github.io/one-forcing/>

Code: <https://github.com/Aurora-edu/One-Forcing>

## Abstract

Recent advances have substantially improved real-time interactive video generation in the autoregressive regime. However, most existing few-step autoregressive video generation methods, often distilled from a corresponding many-step teacher, default to a 4-step sampling configuration, which still incurs considerable latency during deployment and suffers from severe quality degradation when the number of sampling steps is further reduced, particularly in the one-step setting. Trajectory-style consistency distillation methods often produce videos with weak dynamics, while DMD-based approaches, such as Self-Forcing, tend to yield blurry frames. To address this challenge, we propose One-Forcing, a simple yet effective approach which augments the DMD objective with an auxiliary GAN loss for high-quality and efficient one-step video generation. Experiments on VBench show that One-Forcing achieves a total score of 83.76, establishing state-of-the-art performance among one-step causal video generation methods and remaining competitive with strong many-step approaches. We further demonstrate that one-step framewise autoregressive generation can be achieved stably with merely one-third of the training cost of the chunkwise model, a setting that prior methods have failed to achieve successfully.

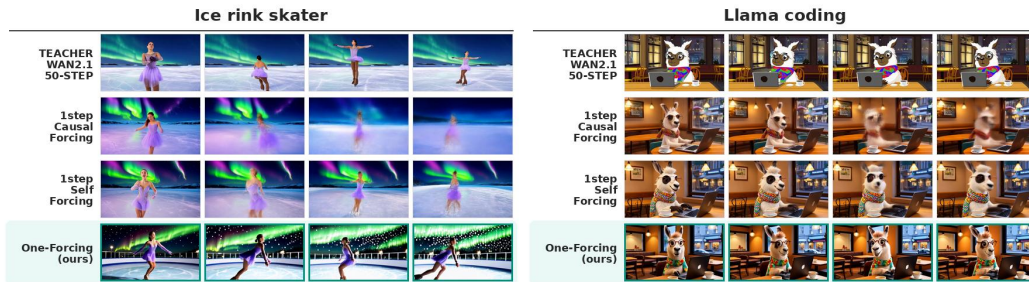


Figure 1: Videos were generated from two prompts using four distinct methods. Wan2.1 teacher uses 50 denoising steps, Causal Forcing, Self Forcing, and One-Forcing use one-step autoregressive sampling. Our method exhibits excellent dynamism and visual quality.

\*Equal contribution.

# 1 Introduction

Diffusion-based video generation has progressed at a remarkable pace. State-of-the-art bidirectional models such as Sora [1], Veo [2], Wan [3], HunyuanVideo [4] and Seedance [5] can now synthesize videos with striking visual fidelity and complex spatiotemporal dynamics. Despite their impressive quality, these models denoise the entire sequence jointly, incurring computational costs that grow prohibitively with video length and precluding real-time or interactive deployment.

Autoregressive video generators address this limitation by producing frames or short temporal blocks in a streaming fashion [6, 7, 8], enabling latency-sensitive applications such as world simulation [9, 10, 11, 12] and interactive game engines [13, 14]. Nevertheless, most causal video systems still require multi-step denoising per block, and this sampling budget remains the primary bottleneck for end-to-end latency. The central question of this paper is whether a causal video generator can preserve strong visual quality and motion dynamics when pushed to the extreme one-step regime.

Existing fast distillation objectives leave a gap in this regime. Consistency-style methods learn endpoint maps along a teacher trajectory and can work well with a small number of steps, but one-step video sampling must approximate the entire high-noise-to-data trajectory with a single jump. We show that Wan [3] video trajectories have a sharp high-noise curvature concentration, unlike the EDM2 [15] image teacher model used as a reference for image consistency distillation, causing video consistency students to lose motion and structure when reduced from a few steps to one step. Distribution Matching Distillation (DMD) offers a different route by matching the teacher distribution through a score-difference estimate of a KL gradient [16]. However, DMD use in causal video distillation remains local to noised generated samples. In autoregressive video, the student rolls out chunks conditioned on its own previous outputs, so blurry or implausible early latents become part of the future context. A score-only fake model can fit the student’s generated distribution without explicitly rejecting samples that remain distinguishable from real video latents.

Built on these insights, we propose One-Forcing, a joint objective that tackles the one-step causal video bottleneck by explicitly unifying Distribution Matching Distillation (DMD) with an adversarial penalty. While DMD efficiently aligns the local score of self-rolled outputs, the adversarial component introduces a much-needed global rejection mechanism to prevent error accumulation across the autoregressive context. Crucially, the discriminator is grounded in actual real video data rather than self-distilled model outputs, ensuring a stable and meaningful density-ratio gradient throughout training. Architecturally, we implement this by reusing the trainable fake-score transformer backbone and appending an auxiliary adversarial head to evaluate the noised latents. On VBench, One-Forcing achieves state-of-the-art one-step performance and remains competitive with strong many-step baselines. We further demonstrate that one-step framewise autoregressive generation can be achieved stably with merely one-third of the training cost of the chunkwise model, a setting that prior methods have failed to achieve successfully. In summary, our contributions are:

- We identify a geometric obstacle to one-step video distillation: video teacher trajectories exhibit sharply concentrated curvature near the high-noise endpoint, unlike image teachers commonly used in consistency distillation. This provides an explanation for why trajectory-based objectives degrade sharply when compressed to a single video generation step.
- We propose One-Forcing, a joint score-matching and adversarial objective that reuses the fake-score transformer backbone as a noised-latent discriminator. This shared architecture provides complementary DMD and GAN gradients without additional network overhead, and grounds the adversarial signal in real data rather than self-distilled model outputs.
- We demonstrate that one-step framewise autoregressive generation, a setting where prior distillation methods fail, converges stably in only 200 steps with our approach, requiring one-third the training cost of chunkwise distillation while achieving higher quality.
- On VBench, One-Forcing achieves *state-of-the-art* one-step causal video generation (83.76 total) and remains competitive with strong many-step approaches.

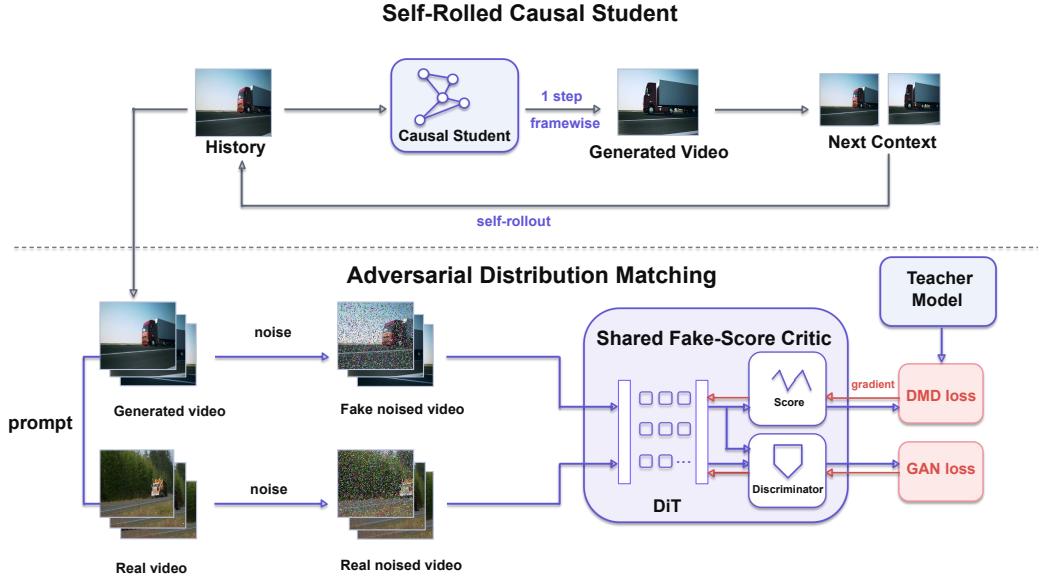


Figure 2: **One-Forcing training framework.** Starting from a one-step causal rollout, One-Forcing optimizes the generated latent distribution with two coupled signals: a DMD gradient from the difference between the trainable fake score and the frozen real score, and an adversarial gradient from a noised-latent discriminator trained against real data. Both signals share the fake-score backbone, so the critic learns denoising and real/fake discrimination in the same latent feature space.

## 2 Related Works

### 2.1 Bidirectional and Autoregressive Video Generation

Current video diffusion models fall into two paradigms. *Bidirectional* models denoise an entire clip with full spatiotemporal attention, achieving strong coherence at the cost of computation that scales quadratically with sequence length [3, 4, 17, 18, 19]. While effective for offline synthesis, these models are impractical for streaming or interactive scenarios that demand low per-frame latency.

Autoregressive (causal) video generators factorize the joint distribution as  $p_\theta(x^{1:K} | c) = \prod_k p_\theta(x^k | x^{<k}, c)$ , so each generated block becomes context for future blocks via a KV cache. This factorization naturally supports real-time streaming: only the current block is denoised while past blocks are fixed in the cache. Self Forcing [7] first demonstrated that training on self-generated context with a holistic video-level loss can close the train-test gap in causal video diffusion. Causal Forcing [8] further showed that using an autoregressive teacher for ODE initialization provably bridges the architectural gap introduced by replacing full attention with causal attention, yielding improvements in dynamics and instruction following. Causal Forcing++ [20] makes this pipeline more scalable by replacing causal ODE initialization with causal consistency distillation, reducing the cost of preparing few-step causal students and enabling frame-wise 2-step autoregressive generation. This initialization-focused direction is complementary to One-Forcing, which targets the one-step distribution matching objective after causal initialization. Other notable systems include CausVid [6], MAGI-1 [21], LongLive [22], Rolling Forcing [23], Infinity-RoPE [24], and Self-Forcing++ [25]. Despite these advances, most causal models still require 4 denoising steps per block; reducing the budget to one step causes pronounced quality degradation.

### 2.2 Diffusion Distillation

Two complementary approaches exist for compressing multi-step diffusion or flow models into fewer steps. One line relies on continuous-time transport trajectories between noise and data. Flow matching [26] and rectified flow transformers [27] learn velocity fields that parameterize such

transport paths, while consistency distillation enforces that a student’s prediction remains invariant along a teacher trajectory, typically a PF-ODE, enabling few-step or one-step generation [28, 29, 30]. Consistency-style and related trajectory-compression methods have scaled well for images [31, 32, 33] and been extended to video [34], but they implicitly assume trajectories that are smooth enough to be faithfully compressed.

Distribution matching distillation (DMD) [16, 35] takes a different route: rather than following a specific teacher path, it estimates a reverse-KL gradient via the difference between a real-distribution score  $s_{\text{real}}$  and a learned fake-distribution score  $s_{\phi}$ , pushing the generator toward the data distribution. Recent video extensions adapt DMD to autoregressive generation with windowed self-rolled sequences [36, 37], reward-weighted distribution matching [38], and diagonal multi-step scheduling [39]. However, DMD’s per-sample score gradient lacks an explicit mechanism to reject outputs that are globally distinguishable from real video, motivating an additional adversarial objective.

### 2.3 Adversarial Training for Video Generation

Generative adversarial networks [40] offer single-pass generation by training a discriminator to separate real and generated samples. Early video GANs produced short clips via 3D convolutions or motion-appearance decompositions [41, 42], and later work improved temporal fidelity with continuous-time generators [43]. However, standalone GANs have not scaled to broad text-conditioned video distributions, so modern systems instead employ adversarial learning as a *post-training* or *distillation* signal on top of diffusion. Adversarial Diffusion Distillation (ADD) [44] pioneered the use of a discriminator to sharpen one-step image outputs. Adversarial Post-Training (APT) [45] extended this to one-step text-to-video generation, demonstrating real-time 24fps synthesis. Most recently, Autoregressive APT (AAPT) [46] combines adversarial training with student-forcing in a causal KV-cache architecture, generating a latent frame per forward pass and streaming minute-long videos at real-time rates. Adversarial Self-Distillation [47] and Phased One-Step Adversarial Equilibrium [48] similarly leverage adversarial objectives for few-step causal video generation. This body of work demonstrates that adversarial supervision remains a potent distributional signal even when the backbone is a diffusion or flow model rather than a standalone GAN.

## 3 Method

### 3.1 Limitations of consistency distillation

The one-step setting removes the iterative correction that normally projects a noisy video latent back to the teacher manifold. This is especially problematic for trajectory-style consistency distillation: with only one model evaluation, the student must replace the entire high-noise-to-data teacher path by a single jump. Standard trajectory-style consistency training enforces adjacent teacher states to share an endpoint prediction:

$$\mathcal{L}_{\text{CM}}(\theta) = \mathbb{E}_{x_t, t} \left[ \left\| f_{\theta}(x_t, t, c) - \text{sg} \left( f_{\bar{\theta}}(\Phi_{\Delta t}(x_t), t - \Delta t, c) \right) \right\|_2^2 \right], \quad (1)$$

where  $\Phi_{\Delta t}$  denotes a teacher step and  $f_{\bar{\theta}}$  is an EMA target. Empirically, most few-step video generation models reduce denoising to at least two steps, while pushing to a single step causes a noticeable performance drop, for example in rCM [33].

Inspired by Transition Matching Distillation and Reflow [36, 49], the analysis measures how much the teacher trajectory deviates from the straight chord connecting its data and noise endpoints. For adjacent teacher states, define

$$C(t_i) = \frac{1}{d} \left\| \frac{x_{t_i} - x_{t_{i-1}}}{t_i - t_{i-1}} - (x_1 - x_0) \right\|_2^2, \quad (2)$$

where  $t = 0$  and  $t = 1$  denote the data and highest-noise endpoints, respectively, and  $d$  is the number of latent coordinates. Thus  $C(t_i)$  measures the per-coordinate squared deviation between the local teacher velocity and the global endpoint chord. Sampling details are provided in Appendix B. Figure 3 shows a sharp difference between image and video teachers. Wan[3] video trajectories concentrate 92.5% of their curvature mass at  $t \geq 0.9$ , while the EDM2 ImageNet-512[15] teacher used by scalable image consistency models has no comparable high-noise spike.

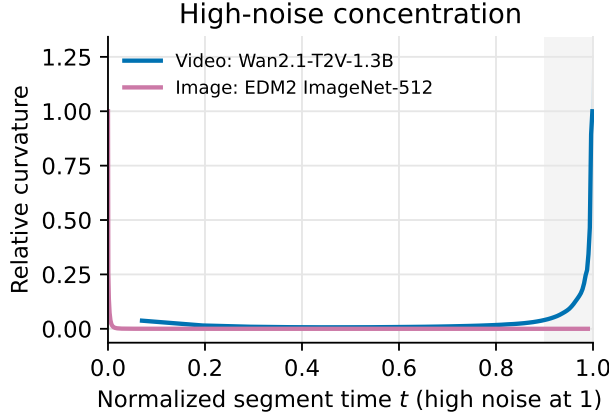


Figure 3: Relative trajectory-curvature profiles show high-noise concentration for Wan video generation but not for EDM2 ImageNet-512 image generation. Each curve is normalized by its own peak.

This provides a geometric explanation for the sharp degradation from few-step to one-step video consistency sampling, whereas image generation models do not suffer from this issue and can thus achieve 1-step generation. A two-step sampler can place an intermediate anchor after the high-noise bend, but a one-step sampler must approximate the dominant nonlinear region at once. Consequently, achieving high-fidelity one-step video generation requires discarding trajectory-based-only objectives in favor of direct output distribution matching. By bypassing the complex intermediate ODE path, methods like DMD avoid the high-noise degradation. Yet, while vanilla DMD excels in one-step image generation, its inherent locality poses a critical threat to autoregressive video rollouts.

### 3.2 Limitations of vanilla DMD

Vanilla DMD matches the generated distribution through a local score-difference signal. For generated samples  $x_\theta = G_\theta(z, c)$ , DMD estimates the reverse-KL gradient

$$\nabla_{\theta} \text{KL}(p_\theta \| p_{\text{data}}) = \mathbb{E}_{x_\theta} [J_\theta(z, c)^\top (\nabla_x \log p_\theta(x_\theta | c) - \nabla_x \log p_{\text{data}}(x_\theta | c))], \quad (3)$$

and implements it with  $s_\phi - s_{\text{real}}$  on noised samples. The key difficulty is that this signal is local to the current generated latents. In one-step image generation, such locality is less problematic because the model produces a single terminal sample. In one-step autoregressive video generation, each predicted latent block is fed back into the causal KV cache and becomes conditioning context for all subsequent blocks. Thus a local score-matching error is not isolated: it is recursively injected into future predictions, where it can compound into blur, weak motion, or temporal drift. This makes distribution-level realism substantially more important than in image DMD2 or image adversarial distillation. We therefore need a critic that can explicitly distinguish noised real and generated video latents, rather than only fitting the fake score around the student’s own rollout distribution.

### 3.3 One-Forcing

One-Forcing keeps the autoregressive generator and DMD objective, but turns the trainable fake-score network into a joint diffusion critic and noised-latent discriminator, as summarized in Figure 2. Following [6, 8], we initialize the causal student by pretraining it on a small set of ODE solution pairs generated by the teacher model. We focus on the framewise one-step setting, where the model emits one latent frame per autoregressive update and immediately feeds that prediction back as causal context for subsequent frames. This setting exposes the student to the same self-generated context used at deployment, while the distributional DMD and adversarial objectives supervise the quality of the resulting rollout.

**Joint score and adversarial critic.** One-Forcing keeps two score networks. The real score  $s_{\text{real}}$  is a frozen bidirectional teacher model. The fake score  $s_\phi$  is a trainable one step autoregressive model.

As in DMD, the fake score is trained to denoise generated latents:

$$\mathcal{L}_{\text{fake}}(\phi) = \mathbb{E}_{x_\theta, t, \epsilon} [\ell_{\text{denoise}}(s_\phi(x_t, t, c), x_\theta, \epsilon, t)], \quad (4)$$

where  $\ell_{\text{denoise}}$  is the flow-matching objective, which trains  $s_\phi$  to predict the velocity target  $\epsilon - x_\theta$  from the noised sample  $x_t$ .

Given a one-step rollout  $x_\theta = G_\theta(z, c)$ , we sample a diffusion timestep  $t$ , form  $x_{\theta, t} = \alpha_t x_\theta + \sigma_t \epsilon$  with  $\epsilon \sim \mathcal{N}(0, I)$ , and evaluate the trainable fake score and frozen real score on the same noised latent. The DMD generator update takes the following stop-gradient form:

$$\mathcal{L}_{\text{DMD}}(\theta) = \frac{1}{2} \mathbb{E}_{x_\theta, t, \epsilon} \left[ \|x_\theta - \text{sg}(x_\theta - [s_\phi(x_{\theta, t}, t, c) - s_{\text{real}}(x_{\theta, t}, t, c)])\|_2^2 \right].$$

This loss passes the fake-minus-real score difference to the generator on the selected autoregressive gradient window, while the fake score itself is trained by the denoising objective above.

The adversarial branch augments the fake-score transformer with a small set of learned register tokens, initialized as trainable embeddings and normalized before use. For each selected transformer layer, one register token is used as a query in a lightweight attention block over that layer’s latent tokens, producing a compact layer-wise critic feature. The features from all selected layers are concatenated and passed through a MLP head  $D_\phi(x_t, t, c)$  to produce a scalar real/fake logit. Real samples  $x_{\text{real}}$  come from the dataset and fake samples  $x_\theta$  come from the current one-step causal generator. Both are noised at critic timestep  $t$ . The non-saturating adversarial losses follow the GAN training framework [40]:

$$\mathcal{L}_G^{\text{adv}}(\theta) = \mathbb{E}_{x_\theta, t} [\text{softplus}(-D_\phi(x_{\theta, t}, t, c))], \quad (5)$$

$$\mathcal{L}_D^{\text{adv}}(\phi) = \mathbb{E}_{x_{\text{real}}, x_\theta, t} [\text{softplus}(-D_\phi(x_{\text{real}, t}, t, c)) + \text{softplus}(D_\phi(x_{\theta, t}, t, c))]. \quad (6)$$

**Training objective.** The generator objective is

$$\mathcal{L}_G = \mathcal{L}_{\text{DMD}} + \lambda_G \mathcal{L}_G^{\text{adv}}, \quad (7)$$

and the critic objective is

$$\mathcal{L}_\phi = \mathcal{L}_{\text{fake}} + \lambda_D \mathcal{L}_D^{\text{adv}}. \quad (8)$$

We use an interleaved update schedule: every training iteration performs one fake-score critic update, and every  $K$  iterations additionally performs one generator update on a separately sampled minibatch. In our default setting  $K = 5$ , giving one generator update for every five critic updates, following the two-time-scale intuition of DMD2 [35]. The full training procedure is summarized in Algorithm 1.

---

#### Algorithm 1 One-Forcing Training

---

**Require:** Generator  $G_\theta$ , fake-score network  $s_\phi$  with discriminator head  $D_\phi$ , frozen real-score  $s_{\text{real}}$ , Dataset  $\mathcal{D}$ , generator interval  $K$ , weights  $\lambda_G, \lambda_D$

- 1: **for** training iteration  $i = 0, 1, \dots$  **do**
  - 2:   **if**  $i \bmod K = 0$  **then**
  - 3:     Sample prompt  $c_G$  from  $\mathcal{D}$
  - 4:     Generate fake samples  $x_\theta \leftarrow G_\theta(\epsilon_G, c_G)$  with one-step causal rollout
  - 5:     Compute  $\mathcal{L}_{\text{DMD}}$  from the normalized score difference  $s_\phi - s_{\text{real}}$  on noised fake samples
  - 6:     Compute  $\mathcal{L}_G^{\text{adv}}$  with  $D_\phi$  on independently noised fake samples
  - 7:     Update  $\theta$ :  $\mathcal{L}_G = \mathcal{L}_{\text{DMD}} + \lambda_G \mathcal{L}_G^{\text{adv}}$
  - 8:   **end if**
  - 9:   Sample a critic minibatch with prompt  $c_\phi$  and real data  $x_{\text{real}}$  from  $\mathcal{D}$
  - 10:   Generate fake samples  $\tilde{x}_\theta \leftarrow G_\theta(\tilde{\epsilon}, c_\phi)$  without generator gradients
  - 11:   Train  $s_\phi$  to denoise noised generated samples, giving  $\mathcal{L}_{\text{fake}}$
  - 12:   Train  $D_\phi$  to classify noised real data as real and noised generated samples as fake, giving  $\mathcal{L}_D^{\text{adv}}$
  - 13:   Update  $\phi$ :  $\mathcal{L}_\phi = \mathcal{L}_{\text{fake}} + \lambda_D \mathcal{L}_D^{\text{adv}}$
  - 14: **end for**
-

Table 1: VBench results for one-step and many-step video generation. Higher is better ( $\uparrow$ ). Entries marked with \* use First-Frame Enhancement (FFE) [47].

Model	#Params	Resolution	NFE	VBench Scores $\uparrow$		
				Total	Quality	Semantic
<i>Many steps</i>						
MAGI-1 [21]	4.5B	832 $\times$ 480	64	79.18	82.04	67.74
Wan2.1 [3]	1.3B	832 $\times$ 480	50	<b>84.26</b>	<b>85.30</b>	<b>80.09</b>
SkyReels-V2 [51]	1.3B	960 $\times$ 540	30	82.67	84.70	74.53
NOVA [52]	0.6B	768 $\times$ 480	25	80.12	80.39	79.05
LTX-Video [53]	1.9B	768 $\times$ 512	20	80.00	82.30	70.79
Pyramid Flow [54]	2B	640 $\times$ 384	20	81.72	84.74	69.62
CausVid [6]	1.3B	832 $\times$ 480	4	81.18	84.41	68.30
Self Forcing [7]	1.3B	832 $\times$ 480	4	83.46	84.77	78.24
<i>1 step</i>						
Self Forcing [7]	1.3B	832 $\times$ 480	1	77.18	79.40	68.34
Causal-Forcing [8]	1.3B	832 $\times$ 480	1	78.39	80.67	69.25
ASD [47]	1.3B	832 $\times$ 480	1*	79.12	81.35	70.19
Ours(chunkwise)	1.3B	832 $\times$ 480	1*	81.60	83.65	73.41
Ours(framewise)	1.3B	832 $\times$ 480	1*	<b>83.76</b>	<b>85.22</b>	<b>77.91</b>

## 4 Experiments

### 4.1 Implementation Details

Similar to prior work [7, 8], the generator is initialized from an ODE initialized checkpoint [8] and uses one denoising timestep per autoregressive block. The trainable fake-score critic uses Wan2.1-T2V-1.3B, while the frozen real-score teacher uses Wan2.1-T2V-14B. Unless otherwise specified, the reported configuration uses 21 frames with 1 latent frame per autoregressive block for the framewise model and 3 latent frames per block for the chunkwise model, a generator update every five critic updates, and non-relativistic adversarial losses. For inference, we follow ASD’s First-Frame Enhancement (FFE) strategy [47]: the first autoregressive block is sampled with four denoising steps, while subsequent blocks use one denoising step. All training is conducted on  $8 \times$  H100 GPUs; inference requires only a single H100. The chunkwise model converges in 750 training steps and the framewise model in only 200 steps, making the distillation highly efficient. Additional implementation details from the final training configuration are provided in Appendix A.

### 4.2 Evaluation

We evaluate text-to-video generation with VBench [50], reporting the official normalized total, quality, and semantic scores to measure both visual fidelity and text-video alignment. Following previous works [7, 8, 22, 47], we compare One-Forcing against both many-step and one-step baselines. For the one-step setting, Self Forcing [7] applies pure DMD distillation that matches the fake-score and real-score distributions without adversarial supervision; Causal-Forcing [8] and ASD [47] which uses adversarial self-distillation where an  $(n+1)$ -step model serves as the “real” target for the  $n$ -step student. All one-step baselines share the same Wan2.1-1.3B backbone for fair comparison. For many-step references, we include Wan2.1 [3], SkyReels-V2 [51], NOVA [52], LTX-Video [53], Pyramid Flow [54], MAGI-1 [21], CausVid [6], and Self Forcing at 4 steps.

### 4.3 Main Results

Table 1 summarizes the results. In the one-step setting, One-Forcing (framewise) achieves a total score of 83.76 with quality 85.22 and semantic 77.91, outperforming all prior one-step causal methods including Self Forcing, Causal-Forcing, and ASD by 4–7 points in total score. Notably, with only a single NFE, One-Forcing *surpasses most many-step baselines* that use 4 to 25 denoising steps, including Self Forcing, CausVid, LTX-Video, Pyramid Flow, and NOVA. The remaining gap to the teacher model, 50-step Wan2.1, is marginal, showing that one-step generation can approach

Table 2: Pairwise human preference for One-Forcing (frameworkise, 1 step) against each baseline. Counts aggregate votes from three annotators on 50 prompts (up to 150 votes per comparison). “Win rate” is the share of decided votes in which One-Forcing is preferred.

Baseline	NFE	Ours wins	Baseline wins	Total	Win rate
Self Forcing 1 step [7]	1	130	17	147	<b>88.4%</b>
ASD [47]	1	139	11	150	<b>92.7%</b>
Self Forcing 4 step [7]	4	32	118	150	21.3%

multi-step quality given an effective distillation objective. We attribute the gain to two design choices: the discriminator is grounded in real data rather than self-distilled outputs, so it provides a stable learning signal even when the generator is far from the data manifold; and the shared fake-score backbone lets the adversarial and score-matching objectives co-evolve on the same feature space without extra parameters. The frameworkise model (1-frame blocks, 200 training steps) also outperforms the chunkwise variant (3-frame blocks, 750 steps) in both total score (83.76 vs. 81.60) and training efficiency: frameworkise generation produces 21 autoregressive blocks per video (vs. 7 for chunkwise), providing  $3\times$  more discriminator feedback per sample, which allows the generator to correct errors at finer temporal granularity and converge in fewer than one-third the training steps. Our chunkwise model (81.60) nonetheless surpasses all existing one-step methods, confirming that the proposed objective is effective across different block granularities.

#### 4.4 Human Study

To complement the automatic VBench evaluation, we conducted a pairwise human preference study comparing One-Forcing (frameworkise, 1 step) against three causal baselines: Self Forcing at 1 step, ASD at 1 step, and Self Forcing at 4 steps. We sampled 50 prompts from the VBench prompt set, stratified by each prompt’s primary VBench dimension to balance motion, appearance, semantic, and consistency-style queries (4–5 prompts each across 11 dimensions: appearance style, color, human action, multiple objects, object class, overall consistency, scene, spatial relationship, subject consistency, temporal flickering, and temporal style). Each prompt yields one A/B pair against each baseline, and every pair is rated independently by three annotators, for up to  $50 \times 3 \times 3 = 450$  votes in total. For every pair we randomize the side that holds the One-Forcing clip with a fixed seed so that left/right position cannot favor one system, and the prompt sample is committed before any votes are collected to avoid cherry-picking. Annotators view both clips auto-playing on loop in adjacent panels and answer

*“Which video is better overall, considering visual quality, motion realism, temporal consistency, and prompt alignment?”*

selecting *left*, *right*, or *tie*.

Table 2 summarizes votes from the three annotators. Compared with the two one-step causal baselines, One-Forcing is clearly preferred: 88.4% over Self Forcing 1-step (130/147 decided votes, with three abstentions) and 92.7% over ASD 1-step (139/150). These large margins are consistent with the VBench results in Table 1, where One-Forcing improves over Self Forcing 1-step and ASD by 6.58 and 4.64 points, respectively. This suggests that, within the one-step setting, VBench largely agrees with human preference.

#### 4.5 Ablation

We ablate the key design choices of One-Forcing using full 16-dimension VBench evaluation with the official normalized scoring. All models are trained on Wan2.1-1.3B with the same data and generate one-step 21-frame videos at  $832 \times 480$ .

**Frameworkise vs. Chunkwise and initialization strategy.** We compare two frameworkise configurations that differ in initialization: causal ODE initialization (row 1) and causal CD initialization (row 2). Both use 1-frame blocks. The ODE-initialized model achieves a higher total score (83.76 vs. 82.36) and substantially stronger dynamic degree (52.76 vs. 23.61), while the CD-initialized variant obtains

Table 3: Ablation study on VBench (16 dimensions, official scoring). Higher is better ( $\uparrow$ ).

Configuration	Quality	Semantic	Total	Dynamic <sup>†</sup>
<b>Ours (Framewise causal init)</b>	<b>85.22</b>	<b>77.91</b>	<b>83.76</b>	<b>52.76</b>
Ours(Framewise CD init)	82.82	80.50	82.36	23.61

<sup>†</sup>Dynamic degree raw score (%). Higher indicates stronger motion.

better semantic scores (80.50 vs. 77.91). We attribute the dynamic advantage of ODE initialization to its training data containing richer motion information from the multi-step ODE trajectory, which provides the generator with a stronger motion prior during distillation. The CD initialization, on the other hand, starts from a model already trained for consistency, which benefits semantic alignment but tends to suppress large motions.

**Forward KL regularization.** We also test a forward-KL-style distillation regularizer that matches the one-step generator output to the teacher ODE endpoint conditioned on the same noisy latent. The probabilistic objective this regularizer approximates is

$$\mathcal{L}_{\text{fkl}} = \mathbb{E}_{x_{t_0}^{\text{ode}}, c} [D_{\text{KL}}(q_{\text{ODE}}(x_0 | x_{t_0}^{\text{ode}}, c) \| p_{\theta}(x_0 | x_{t_0}^{\text{ode}}, t_0, c))], \quad (9)$$

where  $q_{\text{ODE}}$  is represented by the saved ODE trajectory. Our implementation does not estimate this KL directly. Instead, it optimizes a deterministic squared-error surrogate: the generator prediction is regressed to the stored clean endpoint  $x_{\text{tar}}^{\text{ode}}$ ,

$$\widehat{\mathcal{L}}_{\text{fkl}} = \mathbb{E}_{x_{t_0}^{\text{ode}}, x_{\text{tar}}^{\text{ode}}} \|G_{\theta}(x_{t_0}^{\text{ode}}, t_0, c) - x_{\text{tar}}^{\text{ode}}\|_2^2. \quad (10)$$

This squared-error surrogate is added to the DMD and adversarial generator objectives with weight  $\lambda_{\text{fkl}}$ . Adding  $\lambda_{\text{fkl}}=1$  substantially hurts performance: quality drops to 75.03, total score to 74.83, and dynamic degree to 1.30. Relative to the chunkwise baseline (total 81.60), the total score drops by nearly 7 points and dynamics almost vanish. These results suggest that the deterministic squared-error surrogate for forward-KL regularization is poorly aligned with the distributional objectives used by One-Forcing in the one-step setting. The objectives therefore conflict, and the extra anchor suppresses motion rather than improving fidelity.

**Discriminator effectiveness.** We compare the adversarial training dynamics of One-Forcing against ASD [47]. Both methods attach a classification branch to the fake-score backbone operating in noised latent space, but they differ fundamentally in what constitutes the “real” distribution for the discriminator. One-Forcing trains the discriminator on *real data*: noised samples from actual videos in the training set, providing a fixed, high-quality target distribution. ASD instead uses a *self-distillation* target, where the output of an  $(n+1)$ -step model serves as “real” for the  $n$ -step student, meaning the discriminator must distinguish between two imperfect model outputs rather than between generated and genuine data.

Figure 4 plots the discriminator logit gap  $|l_r - l_f|$  over training. One-Forcing maintains a large, actively varying gap ( $\mu=1.53, \sigma=1.20$ ): the distributional distance between generated latents and real data is substantial and evolves as the generator improves, indicating a healthy adversarial dynamic. In contrast, ASD’s logit gap stays near zero ( $\mu=0.001, \max < 0.006$ ) from the very first steps. Because both sides of ASD’s comparison are model-generated latents with minimal distributional difference, the discriminator never receives a meaningful learning signal and effectively collapses. This confirms that grounding the adversarial signal in *real data* is critical for effective GAN-based video distillation.

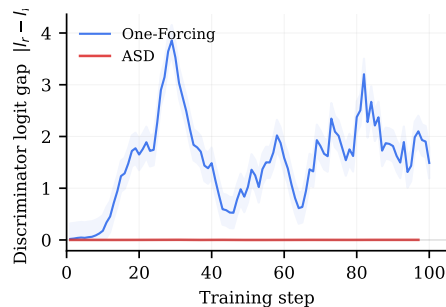


Figure 4: Discriminator logit gap  $|l_r - l_f|$  during training. One-Forcing (blue) maintains a large, varying gap, while ASD (red) stays near zero, confirming a collapsed discriminator.

## 5 Conclusion

We presented One-Forcing, a simple yet effective method that adds an adversarial noised-latent branch to DMD-based causal video distillation by reusing the fake-score backbone as a discriminator. The shared architecture provides density-ratio feedback grounded in real data without extra parameters. We also analyze the failure patterns of previous methods. On VBench, the resulting one-step generator scores 83.76, closing most of the gap to 50-step Wan2.1 (84.26). The framewise variant converges in 200 steps with only one-third the cost of chunkwise training, confirming that stable one-step framewise distillation is achievable with the proposed objective.

## 6 Limitations and Future Work

One-Forcing requires real data as the “real” distribution for the discriminator, which is different from data-free methods such as Self Forcing [7] and ASD [47]. However, these data are already available in standard forcing-like distillation settings where training videos or their precomputed representations are used. For future work, we plan to scale One-Forcing to higher-resolution and longer-duration generation by combining it with efficient attention mechanisms, state-of-the-art long video generation frameworks [22, 23, 24, 25] and larger backbone architectures (e.g., 14B parameters), where the quality of the one-step generator may be further raised. Exploring adaptive step scheduling that dynamically allocates more denoising steps to perceptually complex segments is another promising direction for balancing quality and efficiency. We also plan to extend this work to action-conditioned video generation for faster interactive world modeling [13, 55, 56, 57].

## References

- [1] Tim Brooks, Bill Peebles, Connor Holmes, Will DePue, Yufei Guo, Li Jing, David Schnurr, Joe Taylor, Troy Luhman, Eric Luhman, Clarence Ng, Ricky Wang, and Aditya Ramesh. Video generation models as world simulators. 2024. URL <https://openai.com/index/video-generation-models-as-world-simulators/>.
- [2] Google DeepMind. Veo: a text-to-video generation system. Technical report, Google DeepMind, 2025. URL <https://storage.googleapis.com/deepmind-media/veo/Veo-3-Tech-Report.pdf>.
- [3] Team Wan, Ang Wang, Baole Ai, Bin Wen, Chaojie Mao, Chen-Wei Xie, Di Chen, Fei Wu Yu, Haiming Zhao, Jianxiao Yang, Jianyuan Zeng, Jiayu Wang, Jingfeng Zhang, Jingren Zhou, Jinkai Wang, Jixuan Chen, Kai Zhu, Kang Zhao, Keyu Yan, Lianghua Huang, Mengyang Feng, Ningyi Zhang, Pandeng Li, Pingyu Wu, Ruihang Chu, Ruili Feng, Shiwei Zhang, Siyang Sun, Tao Fang, Tianxing Wang, Tianyi Gui, Tingyu Weng, Tong Shen, Wei Lin, et al. Wan: Open and advanced large-scale video generative models, 2025. URL <https://arxiv.org/abs/2503.20314>.
- [4] Weijie Kong, Qi Tian, Zijian Zhang, Rox Min, Zuozhuo Dai, Jin Zhou, Jiangfeng Xiong, Xin Li, Bo Wu, Jianwei Zhang, Kathrina Wu, Qin Lin, Junkun Yuan, Yanxin Long, Aladdin Wang, Andong Wang, Changlin Li, Duoju Huang, Fang Yang, Hao Tan, Hongmei Wang, Jacob Song, Jiawang Bai, Jianbing Wu, Jinbao Xue, Joey Wang, Kai Wang, Mengyang Liu, Pengyu Li, Shuai Li, Weiyan Wang, Wenqing Yu, Xincheng Deng, Yang Li, Yi Chen, Yutao Cui, Yuanbo Peng, Zhentao Yu, Zhiyu He, Zhiyong Xu, Zixiang Zhou, Zunnan Xu, Yangyu Tao, Qinglin Lu, Songtao Liu, Dax Zhou, Hongfa Wang, Yong Yang, Di Wang, Yuhong Liu, Jie Jiang, and Caesar Zhong. HunyuanVideo: A systematic framework for large video generative models, 2024. URL <https://arxiv.org/abs/2412.03603>.
- [5] Team Seedance, De Chen, Liyang Chen, Xin Chen, Ying Chen, Zhuo Chen, Zhuowei Chen, Feng Cheng, Tianheng Cheng, Yufeng Cheng, Mojie Chi, Xuyan Chi, Jian Cong, Qinpeng Cui, Fei Ding, Qide Dong, et al. Seedance 2.0: Advancing video generation for world complexity, 2026. URL <https://arxiv.org/abs/2604.14148>.
- [6] Tianwei Yin, Qiang Zhang, Richard Zhang, William T. Freeman, Frédo Durand, Eli Shechtman, and Xun Huang. From slow bidirectional to fast autoregressive video diffusion models. In *Proceedings of the IEEE/CVF Conference on Computer Vision and Pattern Recognition (CVPR)*, pages 22963–22974, June 2025. doi: 10.1109/CVPR52734.2025.02138.

- URL [https://openaccess.thecvf.com/content/CVPR2025/html/Yin\\_From\\_Slow\\_Bidirectional\\_to\\_Fast\\_Autoregressive\\_Video\\_Diffusion\\_Models\\_CVPR\\_2025\\_paper.html](https://openaccess.thecvf.com/content/CVPR2025/html/Yin_From_Slow_Bidirectional_to_Fast_Autoregressive_Video_Diffusion_Models_CVPR_2025_paper.html).
- [7] Xun Huang, Zhengqi Li, Guande He, Mingyuan Zhou, and Eli Shechtman. Self forcing: Bridging the train-test gap in autoregressive video diffusion. In D. Belgrave, C. Zhang, H. Lin, R. Pascanu, P. Koniusz, M. Ghassemi, and N. Chen, editors, *Advances in Neural Information Processing Systems*, volume 38, pages 167283–167308. Curran Associates, Inc., 2025. URL [https://proceedings.neurips.cc/paper\\_files/paper/2025/file/f4823f831af67a3ef15e41a85434422a-Paper-Conference.pdf](https://proceedings.neurips.cc/paper_files/paper/2025/file/f4823f831af67a3ef15e41a85434422a-Paper-Conference.pdf).
- [8] Hongzhou Zhu, Min Zhao, Guande He, Hang Su, Chongxuan Li, and Jun Zhu. Causal Forcing: Autoregressive diffusion distillation done right for high-quality real-time interactive video generation, 2026. URL <https://arxiv.org/abs/2602.02214>.
- [9] David Ha and Jürgen Schmidhuber. Recurrent world models facilitate policy evolution. In *Advances in Neural Information Processing Systems*, volume 31, pages 2450–2462. Curran Associates, Inc., 2018. URL <https://proceedings.neurips.cc/paper/2018/hash/2de5d16682c3c35007e4e92982f1a2ba-Abstract.html>.
- [10] Danijar Hafner, Jurgis Pasukonis, Jimmy Ba, and Timothy Lillicrap. Mastering diverse control tasks through world models. *Nature*, 640(8059):647–653, 2025. doi: 10.1038/s41586-025-08744-2. URL <https://doi.org/10.1038/s41586-025-08744-2>.
- [11] Jack Parker-Holder, Philip Ball, Jake Bruce, Vibhavari Dasagi, Kristian Holsheimer, Christos Kaplanis, Alexandre Moufarek, Guy Scully, Jeremy Shar, Jimmy Shi, Stephen Spencer, Jessica Yung, Michael Dennis, Sultan Kenjeyev, Shangbang Long, Vlad Mnih, Harris Chan, Maxime Gazeau, Bonnie Li, Fabio Pardo, Luyu Wang, Lei Zhang, Frederic Besse, Tim Harley, Anna Mitenkova, Jane Wang, Jeff Clune, Demis Hassabis, Raia Hadsell, Adrian Bolton, Satinder Singh, and Tim Rocktäschel. Genie 2: A large-scale foundation world model. Google DeepMind blog, 2024. URL <https://deepmind.google/blog/genie-2-a-large-scale-foundation-world-model/>. Accessed: 2026-05-07.
- [12] Yixuan Zhu, Feng Jiaqi, Wenzhao Zheng, Yuan Gao, Xin Tao, Pengfei Wan, Jiwen Lu, and Jie Zhou. Astra: General interactive world model with autoregressive denoising. In *The Fourteenth International Conference on Learning Representations*, 2026. URL <https://openreview.net/forum?id=8UZpnrxoLG>.
- [13] Jake Bruce, Michael D Dennis, Ashley Edwards, Jack Parker-Holder, Yuge Shi, Edward Hughes, Matthew Lai, Aditi Mavalankar, Richie Steigerwald, Chris Apps, Yusuf Aytar, Sarah Maria Elisabeth Bechtle, Feryal Behbahani, Stephanie C.Y. Chan, Nicolas Heess, Lucy Gonzalez, Simon Osindero, Sherjil Ozair, Scott Reed, Jingwei Zhang, Konrad Zolna, Jeff Clune, Nando De Freitas, Satinder Singh, and Tim Rocktäschel. Genie: Generative interactive environments. In Ruslan Salakhutdinov, Zico Kolter, Katherine Heller, Adrian Weller, Nuria Oliver, Jonathan Scarlett, and Felix Berkenkamp, editors, *Proceedings of the 41st International Conference on Machine Learning*, volume 235 of *Proceedings of Machine Learning Research*, pages 4603–4623. PMLR, 21–27 Jul 2024. URL <https://proceedings.mlr.press/v235/bruce24a.html>.
- [14] Dani Valevski, Yaniv Leviathan, Moab Arar, and Shlomi Fruchter. Diffusion models are real-time game engines. In *The Thirteenth International Conference on Learning Representations*, 2025. URL <https://openreview.net/forum?id=P8pqeEkn1H>.
- [15] Tero Karras, Miika Aittala, Jaakko Lehtinen, Janne Hellsten, Timo Aila, and Samuli Laine. Analyzing and improving the training dynamics of diffusion models. In *Proceedings of the IEEE/CVF Conference on Computer Vision and Pattern Recognition (CVPR)*, pages 24174–24184, June 2024. doi: 10.1109/CVPR52733.2024.02282. URL [https://openaccess.thecvf.com/content/CVPR2024/html/Karras\\_Analyzing\\_and\\_Improving\\_the\\_Training\\_Dynamics\\_of\\_Diffusion\\_Models\\_CVPR\\_2024\\_paper.html](https://openaccess.thecvf.com/content/CVPR2024/html/Karras_Analyzing_and_Improving_the_Training_Dynamics_of_Diffusion_Models_CVPR_2024_paper.html).
- [16] Tianwei Yin, Michaël Gharbi, Richard Zhang, Eli Shechtman, Frédo Durand, William T. Freeman, and Taesung Park. One-step diffusion with distribution matching distillation.

- In *Proceedings of the IEEE/CVF Conference on Computer Vision and Pattern Recognition (CVPR)*, pages 6613–6623, June 2024. doi: 10.1109/CVPR52733.2024.00632. URL [https://openaccess.thecvf.com/content/CVPR2024/html/Yin\\_One-step\\_Diffusion\\_with\\_Distribution\\_Matching\\_Distillation\\_CVPR\\_2024\\_paper.html](https://openaccess.thecvf.com/content/CVPR2024/html/Yin_One-step_Diffusion_with_Distribution_Matching_Distillation_CVPR_2024_paper.html).
- [17] Jonathan Ho, Tim Salimans, Alexey Gritsenko, William Chan, Mohammad Norouzi, and David J. Fleet. Video diffusion models. In S. Koyejo, S. Mohamed, A. Agarwal, D. Belgrave, K. Cho, and A. Oh, editors, *Advances in Neural Information Processing Systems*, volume 35, pages 8633–8646. Curran Associates, Inc., 2022. URL [https://proceedings.neurips.cc/paper\\_files/paper/2022/file/39235c56aef13fb05a6adc95eb9d8d66-Paper-Conference.pdf](https://proceedings.neurips.cc/paper_files/paper/2022/file/39235c56aef13fb05a6adc95eb9d8d66-Paper-Conference.pdf).
- [18] Jonathan Ho, William Chan, Chitwan Saharia, Jay Whang, Ruiqi Gao, Alexey Gritsenko, Diederik P. Kingma, Ben Poole, Mohammad Norouzi, David J. Fleet, and Tim Salimans. Imagen Video: High definition video generation with diffusion models, 2022. URL <https://arxiv.org/abs/2210.02303>.
- [19] Zhuoyi Yang, Jiayan Teng, Wendi Zheng, Ming Ding, Shiyu Huang, Jiazheng Xu, Yuanming Yang, Wenyi Hong, Xiaohan Zhang, Guanyu Feng, Da Yin, Yuxuan Zhang, Weihang Wang, Ye Chen, Bin Xu, Xiaotao Gu, Yuxiao Dong, and Jie Tang. CogVideoX: Text-to-video diffusion models with an expert transformer. In *The Thirteenth International Conference on Learning Representations*, 2025. URL <https://openreview.net/forum?id=LQzN6TRFg9>.
- [20] Min Zhao, Hongzhou Zhu, Kaiwen Zheng, Zihan Zhou, Bokai Yan, Xinyuan Li, Xiao Yang, Chongxuan Li, and Jun Zhu. Causal Forcing++: Scalable few-step autoregressive diffusion distillation for real-time interactive video generation, 2026. URL <https://arxiv.org/abs/2605.15141>.
- [21] Sand.ai, Hansi Teng, Hongyu Jia, Lei Sun, Lingzhi Li, Maolin Li, Mingqiu Tang, Shuai Han, Tianning Zhang, W. Q. Zhang, Weifeng Luo, Xiaoyang Kang, Yuchen Sun, Yue Cao, Yunpeng Huang, Yutong Lin, Yuxin Fang, Zewei Tao, Zheng Zhang, Zhongshu Wang, Zixun Liu, Dai Shi, Guoli Su, Hanwen Sun, Hong Pan, Jie Wang, Jiexin Sheng, Min Cui, Min Hu, Ming Yan, Shucheng Yin, Siran Zhang, Tingting Liu, Xianping Yin, Xiaoyu Yang, Xin Song, Xuan Hu, Yankai Zhang, and Yuqiao Li. MAGI-1: Autoregressive video generation at scale, 2025. URL <https://arxiv.org/abs/2505.13211>.
- [22] Shuai Yang, Wei Huang, Ruihang Chu, Yicheng Xiao, Yuyang Zhao, Xianbang Wang, Muyang Li, Enze Xie, Ying-Cong Chen, Yao Lu, Song Han, and Yukang Chen. LongLive: Real-time interactive long video generation. In *The Fourteenth International Conference on Learning Representations*, 2026. URL <https://openreview.net/forum?id=nCAODkpsPJ>.
- [23] Kunhao Liu, Wenbo Hu, Jiale Xu, Ying Shan, and Shijian Lu. Rolling forcing: Autoregressive long video diffusion in real time. In *The Fourteenth International Conference on Learning Representations*, 2026. URL <https://openreview.net/forum?id=IAyzXjbfwo>.
- [24] Hidir Yesiltepe, Tuna Han Salih Meral, Adil Kaan Akan, Kaan Oktay, and Pinar Yanardag. Infinity-RoPE: Action-controllable infinite video generation emerges from autoregressive self-rollback, 2025. URL <https://arxiv.org/abs/2511.20649>. CVPR 2026.
- [25] Justin Cui, Jie Wu, Ming Li, Tao Yang, Xiaojie Li, Rui Wang, Andrew Bai, Yuanhao Ban, and Cho-Jui Hsieh. Self-forcing++: Towards minute-scale high-quality video generation. In *The Fourteenth International Conference on Learning Representations*, 2026. URL <https://openreview.net/forum?id=DzvPiqh23f>.
- [26] Yaron Lipman, Ricky T. Q. Chen, Heli Ben-Hamu, Maximilian Nickel, and Matthew Le. Flow matching for generative modeling. In *The Eleventh International Conference on Learning Representations*, 2023. URL <https://openreview.net/forum?id=PqvMRDCJT9t>.
- [27] Patrick Esser, Sumith Kulal, Andreas Blattmann, Rahim Entezari, Jonas Müller, Harry Saini, Yam Levi, Dominik Lorenz, Axel Sauer, Frederic Boesel, Dustin Podell, Tim Dockhorn, Zion English, and Robin Rombach. Scaling rectified flow transformers for high-resolution image synthesis. In *Proceedings of the 41st International Conference on Machine Learning*, volume 235 of *Proceedings of Machine Learning Research*, pages 12606–12633. PMLR, 2024. URL <https://proceedings.mlr.press/v235/esser24a.html>.

- [28] Yang Song, Prafulla Dhariwal, Mark Chen, and Ilya Sutskever. Consistency models. In Andreas Krause, Emma Brunskill, Kyunghyun Cho, Barbara Engelhardt, Sivan Sabato, and Jonathan Scarlett, editors, *Proceedings of the 40th International Conference on Machine Learning*, volume 202 of *Proceedings of Machine Learning Research*, pages 32211–32252. PMLR, 23–29 Jul 2023. URL <https://proceedings.mlr.press/v202/song23a.html>.
- [29] Yang Song and Prafulla Dhariwal. Improved techniques for training consistency models. In *The Twelfth International Conference on Learning Representations*, 2024. URL <https://openreview.net/forum?id=WNzy9bRDvG>.
- [30] Cheng Lu and Yang Song. Simplifying, stabilizing and scaling continuous-time consistency models. In *The Thirteenth International Conference on Learning Representations*, 2025. URL <https://openreview.net/forum?id=LyJi5ugyJx>.
- [31] Simian Luo, Yiqin Tan, Longbo Huang, Jian Li, and Hang Zhao. Latent consistency models: Synthesizing high-resolution images with few-step inference, 2023. URL <https://arxiv.org/abs/2310.04378>.
- [32] Kevin Frans, Danijar Hafner, Sergey Levine, and Pieter Abbeel. One step diffusion via shortcut models. In *The Thirteenth International Conference on Learning Representations*, 2025. URL <https://openreview.net/forum?id=0lzB6LnXcS>.
- [33] Kaiwen Zheng, Yuji Wang, Qianli Ma, Huayu Chen, Jintao Zhang, Yogesh Balaji, Jianfei Chen, Ming-Yu Liu, Jun Zhu, and Qinsheng Zhang. Large scale diffusion distillation via score-regularized continuous-time consistency. In *The Fourteenth International Conference on Learning Representations*, 2026. URL <https://openreview.net/forum?id=2uN1M353RI>.
- [34] Zhengyao Lv, Chenyang Si, Tianlin Pan, Zhaoxi Chen, Kwan-Yee K. Wong, Yu Qiao, and Ziwei Liu. Dual-expert consistency model for efficient and high-quality video generation. In *Proceedings of the IEEE/CVF International Conference on Computer Vision (ICCV)*, pages 14983–14993, October 2025. URL [https://openaccess.thecvf.com/content/ICCV2025/html/Lv\\_Dual-Expert\\_Consistency\\_Model\\_for\\_Efficient\\_and\\_High-Quality\\_Video\\_Generation\\_ICCV\\_2025\\_paper.html](https://openaccess.thecvf.com/content/ICCV2025/html/Lv_Dual-Expert_Consistency_Model_for_Efficient_and_High-Quality_Video_Generation_ICCV_2025_paper.html).
- [35] Tianwei Yin, Michaël Gharbi, Taesung Park, Richard Zhang, Eli Shechtman, Frédo Durand, and William T. Freeman. Improved distribution matching distillation for fast image synthesis. In A. Globerson, L. Mackey, D. Belgrave, A. Fan, U. Paquet, J. Tomczak, and C. Zhang, editors, *Advances in Neural Information Processing Systems*, volume 37, pages 47455–47487. Curran Associates, Inc., 2024. doi: 10.52202/079017-1505. URL [https://proceedings.neurips.cc/paper\\_files/paper/2024/file/54dcf25318f9de5a7a01f0a4125c541e-Paper-Conference.pdf](https://proceedings.neurips.cc/paper_files/paper/2024/file/54dcf25318f9de5a7a01f0a4125c541e-Paper-Conference.pdf).
- [36] Weili Nie, Julius Berner, Nanye Ma, Chao Liu, Saining Xie, and Arash Vahdat. Transition matching distillation for fast video generation, 2026. URL <https://arxiv.org/abs/2601.09881>.
- [37] Xingtong Ge, Yi Zhang, Yushi Huang, Dailan He, Xiahong Wang, Bingqi Ma, Guanglu Song, Yu Liu, and Jun Zhang. Salt: Self-consistent distribution matching with cache-aware training for fast video generation, 2026. URL <https://arxiv.org/abs/2604.03118>.
- [38] Yunhong Lu, Yanhong Zeng, Haobo Li, Hao Ouyang, Qiuyu Wang, Ka Leong Cheng, Jiapeng Zhu, Hengyuan Cao, Zhipeng Zhang, Xing Zhu, Yujun Shen, and Min Zhang. Reward forcing: Efficient streaming video generation with rewarded distribution matching distillation, 2025. URL <https://arxiv.org/abs/2512.04678>.
- [39] Jinxiu Liu, Xuanming Liu, Kangfu Mei, Yandong Wen, Ming-Hsuan Yang, and Weiyang Liu. Streaming autoregressive video generation via diagonal distillation. In *The Fourteenth International Conference on Learning Representations*, 2026. URL <https://openreview.net/forum?id=X7YW6STzeL>.
- [40] Ian J. Goodfellow, Jean Pouget-Abadie, Mehdi Mirza, Bing Xu, David Warde-Farley, Sherjil Ozair, Aaron Courville, and Yoshua Bengio. Generative adversarial nets. In Zoubin Ghahramani, Max Welling, Corinna Cortes, Neil D. Lawrence, and Kilian Q. Weinberger, editors, *Advances*

- in *Neural Information Processing Systems*, volume 27, pages 2672–2680. Curran Associates, Inc., 2014. URL [https://proceedings.neurips.cc/paper\\_files/paper/2014/file/f033ed80deb0234979a61f95710dbe25-Paper.pdf](https://proceedings.neurips.cc/paper_files/paper/2014/file/f033ed80deb0234979a61f95710dbe25-Paper.pdf).
- [41] Carl Vondrick, Hamed Pirsiavash, and Antonio Torralba. Generating videos with scene dynamics. In *Advances in Neural Information Processing Systems*, volume 29, pages 613–621. Curran Associates, Inc., 2016. URL [https://proceedings.neurips.cc/paper\\_files/paper/2016/file/04025959b191f8f9de3f924f0940515f-Paper.pdf](https://proceedings.neurips.cc/paper_files/paper/2016/file/04025959b191f8f9de3f924f0940515f-Paper.pdf).
- [42] Sergey Tulyakov, Ming-Yu Liu, Xiaodong Yang, and Jan Kautz. MoCoGAN: Decomposing motion and content for video generation. In *Proceedings of the IEEE Conference on Computer Vision and Pattern Recognition (CVPR)*, pages 1526–1535, June 2018. doi: 10.1109/CVPR.2018.00165. URL [https://openaccess.thecvf.com/content\\_cvpr\\_2018/html/Tulyakov\\_MoCoGAN\\_Decomposing\\_Motion\\_CVPR\\_2018\\_paper.html](https://openaccess.thecvf.com/content_cvpr_2018/html/Tulyakov_MoCoGAN_Decomposing_Motion_CVPR_2018_paper.html).
- [43] Ivan Skorokhodov, Sergey Tulyakov, and Mohamed Elhoseiny. StyleGAN-V: A continuous video generator with the price, image quality and perks of StyleGAN2. In *Proceedings of the IEEE/CVF Conference on Computer Vision and Pattern Recognition (CVPR)*, pages 3626–3636, June 2022. URL [https://openaccess.thecvf.com/content/CVPR2022/html/Skorokhodov\\_StyleGAN-V\\_A\\_Continuous\\_Video\\_Generator\\_With\\_the\\_Price\\_Image\\_Quality\\_CVPR\\_2022\\_paper.html](https://openaccess.thecvf.com/content/CVPR2022/html/Skorokhodov_StyleGAN-V_A_Continuous_Video_Generator_With_the_Price_Image_Quality_CVPR_2022_paper.html).
- [44] Axel Sauer, Dominik Lorenz, Andreas Blattmann, and Robin Rombach. Adversarial diffusion distillation. In *Computer Vision – ECCV 2024*, volume 15144 of *Lecture Notes in Computer Science*, pages 87–103. Springer, 2024. doi: 10.1007/978-3-031-73016-0\_6. URL [https://doi.org/10.1007/978-3-031-73016-0\\_6](https://doi.org/10.1007/978-3-031-73016-0_6).
- [45] Shanchuan Lin, Xin Xia, Yuxi Ren, Ceyuan Yang, Xuefeng Xiao, and Lu Jiang. Diffusion adversarial post-training for one-step video generation. In Aarti Singh, Maryam Fazel, Daniel Hsu, Simon Lacoste-Julien, Felix Berkenkamp, Tegan Maharaj, Kiri Wagstaff, and Jerry Zhu, editors, *Proceedings of the 42nd International Conference on Machine Learning*, volume 267 of *Proceedings of Machine Learning Research*, pages 37959–37974. PMLR, 13–19 Jul 2025. URL <https://proceedings.mlr.press/v267/lin25m.html>.
- [46] Shanchuan Lin, Ceyuan Yang, Hao He, Jianwen Jiang, Yuxi Ren, Xin Xia, Yang Zhao, Xuefeng Xiao, and Lu Jiang. Autoregressive adversarial post-training for real-time interactive video generation. In D. Belgrave, C. Zhang, H. Lin, R. Pascanu, P. Koniusz, M. Ghassemi, and N. Chen, editors, *Advances in Neural Information Processing Systems*, volume 38, pages 41061–41086. Curran Associates, Inc., 2025. URL [https://proceedings.neurips.cc/paper\\_files/paper/2025/file/3a9468a918fc65dc9ce7b7bd99f4f0ef-Paper-Conference.pdf](https://proceedings.neurips.cc/paper_files/paper/2025/file/3a9468a918fc65dc9ce7b7bd99f4f0ef-Paper-Conference.pdf).
- [47] Yongqi Yang, Huayang Huang, Xu Peng, Xiaobin Hu, Donghao Luo, Jiangning Zhang, Chengjie Wang, and Yu Wu. Towards one-step causal video generation via adversarial self-distillation. In *The Fourteenth International Conference on Learning Representations*, 2026. URL <https://openreview.net/forum?id=P300fNmnWa>.
- [48] Jiaxiang Cheng, Bing Ma, Xuhua Ren, Hongyi Henry Jin, Kai Yu, Peng Zhang, Wenyue Li, Yuan Zhou, Tianxiang Zheng, and Qinglin Lu. Phased one-step adversarial equilibrium for video diffusion models. *Proceedings of the AAAI Conference on Artificial Intelligence*, 40(5): 3237–3245, March 2026. doi: 10.1609/aaai.v40i5.37318. URL <https://ojs.aaai.org/index.php/AAAI/article/view/37318>.
- [49] Xingchao Liu, Chengyue Gong, and Qiang Liu. Flow straight and fast: Learning to generate and transfer data with rectified flow. In *The Eleventh International Conference on Learning Representations*, 2023. URL <https://openreview.net/forum?id=XVjTT1nw5z>.
- [50] Ziqi Huang, Yinan He, Jiashuo Yu, Fan Zhang, Chenyang Si, Yuming Jiang, Yuanhan Zhang, Tianxing Wu, Qingyang Jin, Nattapol Chanpaisit, Yaohui Wang, Xinyuan Chen, Limin Wang, Dahua Lin, Yu Qiao, and Ziwei Liu. VBench: Comprehensive benchmark suite for video generative models. In *Proceedings of the IEEE/CVF Conference on Computer Vision and Pattern Recognition (CVPR)*, pages 21807–21818, June 2024. doi: 10.1109/CVPR52733.2024.02060. URL [https://openaccess.thecvf.com/content/CVPR2024/html/Huang\\_VBench\\_](https://openaccess.thecvf.com/content/CVPR2024/html/Huang_VBench_)

Comprehensive\_Benchmark\_Suite\_for\_Video\_Generative\_Models\_CVPR\_2024\_paper.html.

- [51] Guibin Chen, Dixuan Lin, Jiangping Yang, Chunze Lin, Junchen Zhu, Mingyuan Fan, Hao Zhang, Sheng Chen, Zheng Chen, Chengcheng Ma, Weiming Xiong, Wei Wang, Nuo Pang, Kang Kang, Zhiheng Xu, Yuzhe Jin, Yupeng Liang, Yubing Song, Peng Zhao, Boyuan Xu, Di Qiu, Debang Li, Zhengcong Fei, Yang Li, and Yahui Zhou. SkyReels-V2: Infinite-length film generative model, 2025. URL <https://arxiv.org/abs/2504.13074>.
- [52] Haoge Deng, Ting Pan, Haiwen Diao, Zhengxiong Luo, Yufeng Cui, Huchuan Lu, Shiguang Shan, Yonggang Qi, and Xinlong Wang. Autoregressive video generation without vector quantization. In *The Thirteenth International Conference on Learning Representations*, 2025. URL <https://openreview.net/forum?id=JE9tCwe3lp>.
- [53] Yoav HaCohen, Nisan Chiprut, Benny Brazowski, Daniel Shalem, Dudu Moshe, Eitan Richardson, Eran Levin, Guy Shiran, Nir Zabari, Ori Gordon, Poriya Panet, Sapir Weissbuch, Victor Kulikov, Yaki Bitterman, Zeev Melumian, and Ofir Bibi. LTX-Video: Realtime video latent diffusion, 2024. URL <https://arxiv.org/abs/2501.00103>.
- [54] Yang Jin, Zhicheng Sun, Ningyuan Li, Kun Xu, Kun Xu, Hao Jiang, Nan Zhuang, Quzhe Huang, Yang Song, Yadong Mu, and Zhouchen Lin. Pyramidal flow matching for efficient video generative modeling. In *The Thirteenth International Conference on Learning Representations*, 2025. URL <https://openreview.net/forum?id=66NzcRQu0q>.
- [55] Philip J. Ball, Jakob Bauer, Frank Belletti, Bethanie Brownfield, Ariel Ephrat, Shlomi Fruchter, Agrim Gupta, Kristian Holsheimer, Aleksander Holynski, Jiri Hron, Christos Kaplanis, Marjorie Limont, Matt McGill, Yanko Oliveira, Jack Parker-Holder, Frank Perbet, Guy Scully, Jeremy Shar, Stephen Spencer, Omer Tov, Ruben Villegas, Emma Wang, Jessica Yung, Cip Baetu, Jordi Berbel, David Bridson, Jake Bruce, Gavin Buttimore, Sarah Chakera, Bilva Chandra, Paul Collins, Alex Cullum, Bogdan Damoc, Vibha Dasagi, Maxime Gazeau, Charles Gbadamosi, Woohyun Han, Ed Hirst, Ashyana Kachra, Lucie Kerley, Kristian Kjems, Eva Knoepfel, Vika Koriakin, Jessica Lo, Cong Lu, Zeb Mehring, Alex Moufarek, Henna Nandwani, Valeria Oliveira, Fabio Pardo, Jane Park, Andrew Pierson, Ben Poole, Helen Ran, Tim Salimans, Manuel Sanchez, Igor Saprykin, Amy Shen, Sailesh Sidhwani, Duncan Smith, Joe Stanton, Hamish Tomlinson, Dimple Vijaykumar, Luyu Wang, Piers Wingfield, Nat Wong, Keyang Xu, Christopher Yew, Nick Young, Vadim Zubov, Douglas Eck, Dumitru Erhan, Koray Kavukcuoglu, Demis Hassabis, Zoubin Ghahramani, Raia Hadsell, Aäron van den Oord, Inbar Mosseri, Adrian Bolton, Satinder Singh, and Tim Rocktäschel. Genie 3: A new frontier for world models. Google DeepMind blog, 2025. URL <https://deepmind.google/discover/blog/genie-3-a-new-frontier-for-world-models/>. Accessed: 2026-05-07.
- [56] Wenqiang Sun, Haiyu Zhang, Haoyuan Wang, Junta Wu, Zehan Wang, Zhenwei Wang, Yunhong Wang, Jun Zhang, Tengfei Wang, and Chunchao Guo. WorldPlay: Towards long-term geometric consistency for real-time interactive world modeling, 2025. URL <https://arxiv.org/abs/2512.14614>.
- [57] Yifan Zhang, Chunli Peng, Boyang Wang, Puyi Wang, Qingcheng Zhu, Fei Kang, Biao Jiang, Zedong Gao, Eric Li, Yang Liu, and Yahui Zhou. Matrix-game: Interactive world foundation model, 2025. URL <https://arxiv.org/abs/2506.18701>.

## A Details of Implementations

Our implementation is based on the Causal Forcing codebase [8] and the Wan2.1 model family [3]. The reported framewise One-Forcing model is initialized from an ODE-trained causal model. The real-score network is a frozen bidirectional Wan2.1-T2V-14B model, and the trainable fake-score network is initialized from Wan2.1-T2V-1.3B. We reuse the fake-score backbone as the adversarial discriminator by adding register tokens, lightweight attention blocks, and a classification head to selected transformer layers. No decoded-frame or video-level discriminator is used.

**Noise schedule and model parameterization.** Following Wan2.1, we use a flow-matching scheduler. For a sampled timestep  $t \in [0, 1000]$ , the shifted noise level is

$$\sigma_t = \frac{k(t/1000)}{1 + (k-1)(t/1000)},$$

with shift factor  $k = 5$  for generator rollouts and for the DMD/GAN critic timestep sampling. The forward corruption process is

$$x_t = (1 - \sigma_t)x_0 + \sigma_t\epsilon, \quad \epsilon \sim \mathcal{N}(0, I),$$

and the flow-prediction target is  $\epsilon - x_0$ . During generation, the model predicts  $v_\theta(x_t, t, c)$  and converts it to a clean latent estimate by  $\hat{x}_0 = x_t - \sigma_t v_\theta(x_t, t, c)$ . Training rollouts use a single denoising timestep per autoregressive block.

**Data and prompt processing.** The distillation stage uses precomputed training data. Each training example contains a text prompt and the corresponding real data sample; raw videos are not decoded or reloaded during this stage. The adversarial real samples are drawn from this dataset, while fake samples are produced by the current one-step causal generator. The reported framewise model is trained on 21 latent frames with spatial latent size  $60 \times 104$  and 16 latent channels, corresponding to  $832 \times 480$  video generation. Text embeddings are computed with the frozen Wan text encoder, and classifier-free guidance uses the standard Wan negative prompt. For VBench evaluation, we similarly rewrite the test prompts using Qwen/Qwen2.5-7B-Instruct following previous works [7, 25].

**Training details.** We train the fake-score critic with the flow denoising objective on generated latents and train the adversarial branch to distinguish noised real data from noised generated samples. Each training iteration performs one critic update; every five iterations, we additionally update the generator on a separately sampled minibatch using the DMD surrogate and the adversarial generator loss. For DMD, the real-score model is evaluated with classifier-free guidance scale 5.0, while the fake-score model is evaluated without classifier-free guidance. The DMD gradient is normalized by the average absolute real-score residual. We use AdamW for both generator and critic, mixed precision, gradient checkpointing, and full-shard FSDP. The reported framewise training run uses 8 NVIDIA H100 GPUs with a per-GPU batch size of 1.

**Inference details.** The reported framewise model generates one latent frame per autoregressive block. For the one-step setting, subsequent autoregressive blocks use one denoising update. Following [47], the first block is generated with a short four-step warm-up schedule to initialize the KV cache before one-step streaming continues. Unless otherwise specified, videos are decoded at  $832 \times 480$  resolution and 16 FPS.

Table 4: Training hyperparameters for the reported framewise One-Forcing configuration.

Hyperparameter	Value
Generator initialization	ODE-trained Causal model
Generator / real score / fake score	Wan2.1-T2V-1.3B / Wan2.1-T2V-14B / Wan2.1-T2V-1.3B
Objective	Flow denoising for fake score; DMD + noised-latent GAN for generator
Training frames	21 latent frames, $16 \times 60 \times 104$ per frame
Frames per autoregressive block	1
Training rollout steps per block	1
Guidance scale	5.0 for generator and real-score CFG; 0.0 for fake-score CFG
Timestep range and shift	1000 training timesteps; shift factor 5.0 for sampled DMD/GAN timesteps
Update schedule	One critic update per iteration; one generator update every five iterations
Optimizer	AdamW, $\beta_1 = 0, \beta_2 = 0.999$ , weight decay 0.01
Learning rates	$1.0 \times 10^{-5}$ for generator and fake-score critic
Batch size	1 per GPU on 8 GPUs
EMA	Decay 0.99, starting after 50 iterations
GAN branch	Layers {21, 29}, 2 registers, 1536 feature dim, 2048 FFN dim, 12 heads
GAN loss	Non-relativistic logistic loss, $\lambda_G = \lambda_D = 0.03$
Discriminator regularization	None
Systems	Mixed precision, gradient checkpointing, full-shard FSDP, activation CPU offload
Convergence steps	200 iterations

## B Trajectory Curvature Analysis Details

This appendix provides the sampling and robustness details for the trajectory-curvature calculation in Equation 2. The video comparison uses 100 50-step Wan2.1-T2V-1.3B[3] trajectories with diverse motion and scene prompts, shift 8, classifier-free guidance 6, and one deterministic seed per prompt. The image-domain comparison uses eight 256-step trajectories from the official EDM2 [15] ImageNet-512 teacher, matching the teacher family used by scalable consistency models [30]. EDM2 noise levels are normalized so  $t = 1$  is the highest-noise endpoint.

The high-noise concentration is stable across prompts: per-prompt estimates give  $92.49\% \pm 0.13\%$  curvature mass at  $t \geq 0.9$  (mean  $\pm$  SEM; 95% bootstrap CI  $[92.24, 92.73]\%$ ) and a high-noise/mid-noise ratio of  $33.1 \pm 0.7$  (95% bootstrap CI  $[31.8, 34.4]$ ). A temporal-difference version of the same metric, which removes static appearance and emphasizes motion structure, still places 88.6% of the curvature mass at  $t \geq 0.9$  with a high/mid ratio of 19.3.

## C Training Loss Curves

Figure 5 compares the training loss curves of our One-Forcing and ASD[47] over the first 100 steps. Both methods start from an ODE-initialized generator checkpoint. Panel (a) shows the DMD loss, which drives the score-matching component; both methods exhibit similar initial magnitudes, though One-Forcing stabilizes at a lower level. Panel (b) reveals the generator GAN loss: One-Forcing’s loss varies actively as the discriminator provides meaningful gradients, whereas ASD’s GAN loss flatlines at  $\ln 2 \cdot 0.01 \approx 0.0069$  throughout training. Panels (c) and (d) show the critic and discriminator losses, respectively; One-Forcing’s discriminator loss decreases over training as it learns to distinguish real from fake, while ASD’s discriminator loss remains constant.

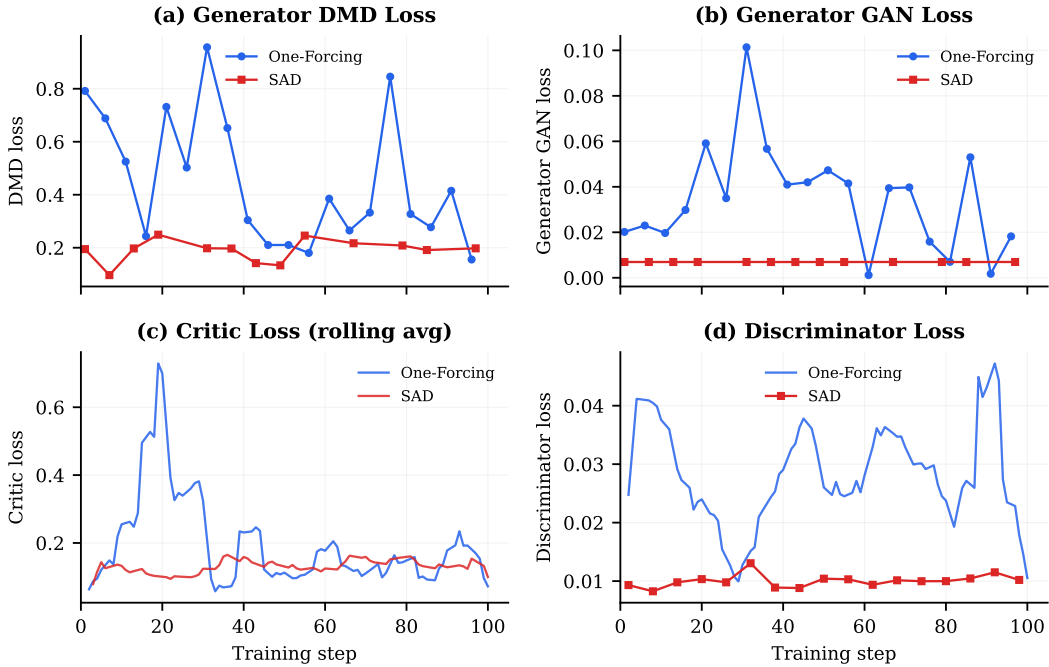


Figure 5: Training loss curves for One-Forcing (blue) and ASD (red) over the first 100 steps. (a) DMD loss. (b) Generator GAN loss. (c) Critic loss (rolling average). (d) Discriminator loss.

## D VBench Scores Across All Dimensions

Following the evaluation visualization style of Self Forcing, Figure 6 expands the full 16-dimensional VBench profile for the Table 1 entries with available per-dimension records: One-Forcing (framewise),

Causal-Forcing 1-step[8], CausVID 4-step[6], ASD[47], Self Forcing DMD 1-step[7], and Self Forcing DMD 4-step. One-Forcing improves over the one-step causal baselines in the aggregate score and shows stronger object, spatial-relation, scene, and dynamic-degree performance than ASD, Causal-Forcing, and one-step Self Forcing, while keeping high temporal smoothness. Compared with four-step Self Forcing, One-Forcing has a higher normalized VBench total and quality score, with gains in dynamic degree and several object/action/scene dimensions, while remaining slightly lower on color, imaging quality, and some consistency-style dimensions.

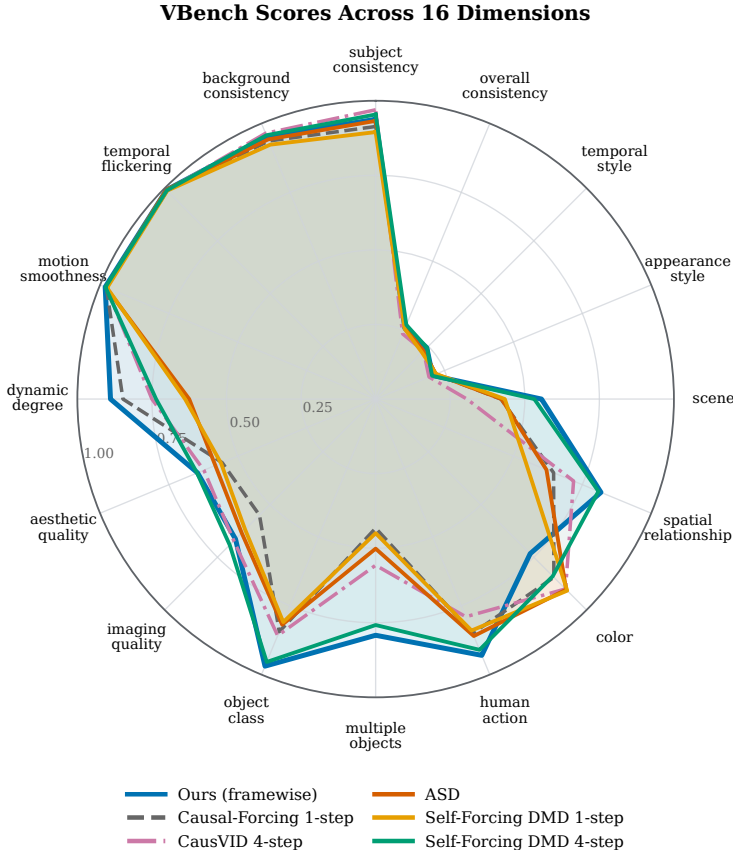


Figure 6: VBench scores across all 16 dimensions for selected Table 1 entries. Higher radial values indicate better normalized VBench sub-metric scores.

### E Broader Societal Impact

Generative modeling, particularly for videos, carries substantial potential for misuse. High-quality video generation can be used to create misleading or fabricated media, amplify disinformation, impersonate individuals, or reinforce harmful stereotypes and social biases present in the training data. These risks are especially important for real-time and low-latency systems, since reducing the computational cost of video synthesis also lowers one practical barrier to large-scale misuse.

At the same time, efficient autoregressive video generation can support beneficial applications such as creative content production, accessibility tools, rapid prototyping, simulation, and interactive world modeling. We therefore view responsible deployment as essential. Practical safeguards should include dataset and prompt filtering, provenance tracking, watermarking or content credentials, synthetic-media detection, clear disclosure of generated content, and policy constraints for sensitive domains. We encourage future work to study safety mechanisms alongside improvements in generation quality and inference speed.